

Optically stimulated luminescence dating at Rose Cottage Cave

Marc Pienaar^{a*}, Stephan Woodborne^a and Lyn Wadley^b

Six optically stimulated luminescence (OSL) dates are compared with stratigraphically associated ¹⁴C dates from Rose Cottage Cave. The OSL dates overlap the accepted ¹⁴C chronology except for one sample that overestimates the expected age by approximately 30%. A single-grain analysis demonstrates that the testing procedure for feldspar fails to reject single aliquots containing feldspar and the overestimate of age is attributed to this. Seven additional luminescence dates for the Middle Stone Age layers combined with the ¹⁴C chronology establish the terminal Middle Stone Age deposits at 27 000 years ago, while stone tool assemblages that are transitional between the Middle Stone Age and the Late Stone Age are dated to between 27 000 years and 20 000 years ago. Although there are inconsistencies in the Middle Stone Age dates, the results suggest that the Howiesons Poort at Rose Cottage Cave dates to between 70 000 years and 60 000 years ago.

Introduction

Much of the rich archaeological heritage in southern Africa is older than 50 000 years, which is the limit of the ubiquitous ¹⁴C dating technique. In order to make appropriate inter-site comparisons of artefactual evidence, and further to compare the trajectory of human adaptation with external factors such as changing climates, it is necessary to establish a reliable chronological framework. Optically stimulated luminescence (OSL) dating has become one of the foremost techniques in establishing this framework. OSL is based on the build-up and release of radiation energy in crystalline minerals, typically quartz. The charge build-up manifests as electrons, mobilized in the quartz matrix by environmental radiation, which populate pre-existing energy minima that are called 'traps'. OSL dates represent the time since electron traps within the quartz grains were previously emptied or bleached by heating or exposure to sunlight. The rate at which traps are repopulated is determined by the environmental dose rate expressed in Gy/kyr. The equivalent dose (D_e) of the sample is divided by the dose rate to calculate the age. Luminescence techniques applied to quartz can be used to obtain depositional ages up to 200 000 years in certain environments.¹

Several criteria need to be met in order to achieve accurate OSL results. The measured aliquots should comprise quartz grains only, and should not contain grains of different ages that might have come about through mixing of the sediments or *in situ* spall decomposition. Mixing of sediments also may occur during sampling when several depositional layers are included in the sample either as a result of the fine nature of the layering, or because of complex, non-horizontal stratification when sampling sections. The zeroing event should also adequately reset the OSL signal in order to avoid the inclusion of quartz grains with residual signals.^{2,3} In addition, the measured dose rate must

represent the average dose rate through time. The widely used laboratory procedure for measuring D_e in quartz grains is called the single-aliquot regenerative-dose (SAR) protocol.⁴ Strict rejection criteria are applied to exclude mixed samples, and in order to ensure that adequate bleaching occurred. If these criteria are satisfied, then the accuracy of the method is determined by the accuracy of the dose rate determination. Several factors influence the dose rate determination. These range from the accuracy with which the moisture content can be established for the depositional history of the sample to assumptions made in the dose rate measurement.

At Rose Cottage Cave (RCC), in the eastern Free State, South Africa, sediments are assumed to have been deposited by fluvial action, wind and erosion of the cave roof and wall material.^{5,6} This scenario suggests the possibility of partial bleaching of the OSL signal at the time of deposition as well as the inclusion of populations of quartz of different ages in any layer. The implicit fluctuation in water content in the cave has implications both for the mobilization of radioactive elements that will lead to changes in the dose rate, and also variability in the attenuation of the radiation flux in the sediment. This scenario is typical of many cave sequences from which Middle Stone Age (MSA) sediments have been excavated, and caution is required in applying the OSL dating technique. Since RCC sediments younger than 50 000 years have one of the best ¹⁴C chronologies of all the archaeological sites in southern Africa,⁵⁻¹⁶ and a comparison can be made between the two techniques, this allows for the testing of the accuracy of the OSL dating technique in a problematic environment.

OSL dating at Rose Cottage Cave

Several luminescence studies using a range of different techniques have been carried out at Rose Cottage Cave. The techniques include infrared stimulated luminescence (IRSL),¹⁷ thermoluminescence (TL),^{17,18} and, more recently, OSL using the SAR protocol.¹⁶ The main advancement of the SAR protocol over previous luminescence methods is the ability to correct for sensitivity changes during measurement cycles. It is assumed that the signal from a fixed test dose (T_x) uses the same electron traps responsible for the OSL signal (L_x). The OSL response to a test dose is measured between each regenerative OSL measurement to provide a quantifiable indication of sensitivity change. Murray and Wintle⁴ suggested that the relationship between the OSL test dose and the OSL regenerative dose must be linear for sensitivity to be adequately corrected.¹⁹ Fourteen sediment samples from RCC were subjected to the standard SAR⁴ luminescence dating protocol. A total of eight of these samples (RCC 6-10, 18, 19, 21) were dated in Pretoria and six (RCC 11-16) were analysed at Risø, Denmark, by A.S. Murray.¹⁶ Of the samples, six have finite ¹⁴C dates from the associated layers. Samples without associated ¹⁴C dates span the pre-Howiesons Poort, Howiesons Poort, and post-Howiesons Poort Middle Stone Age layers at the site (Fig. 1).

The layers from which luminescence samples were collected include six that have associated radiocarbon dates (Fig. 1). Each layer was discretely excavated and predominantly charcoal, but occasionally bone, were radiocarbon dated. The 'orange sand' comprises approximately a metre of deposit that has low artefact density, but it is nevertheless not entirely homogeneous as it retains some sedimentary features.¹⁶ It is difficult to reconstruct the provenance of the original samples submitted for analysis by Butzer and Mason, and so we rely on the analyses obtained by Wadley (see Fig. 1 and associated references)

All luminescence samples were taken in dark conditions and subject to quartz isolation pre-treatment in a dark laboratory. Samples were treated with concentrated hydrochloric acid to

^aEcosystems Processes and Dynamics, CSIR, P.O. Box 395, Pretoria 0001, South Africa.

^bSchool of Geography, Archaeology and Environmental Studies, University of the Witwatersrand, Private Bag 3, WITS 2050, South Africa.

*Author for correspondence. E-mail: mpienaar@csir.co.za

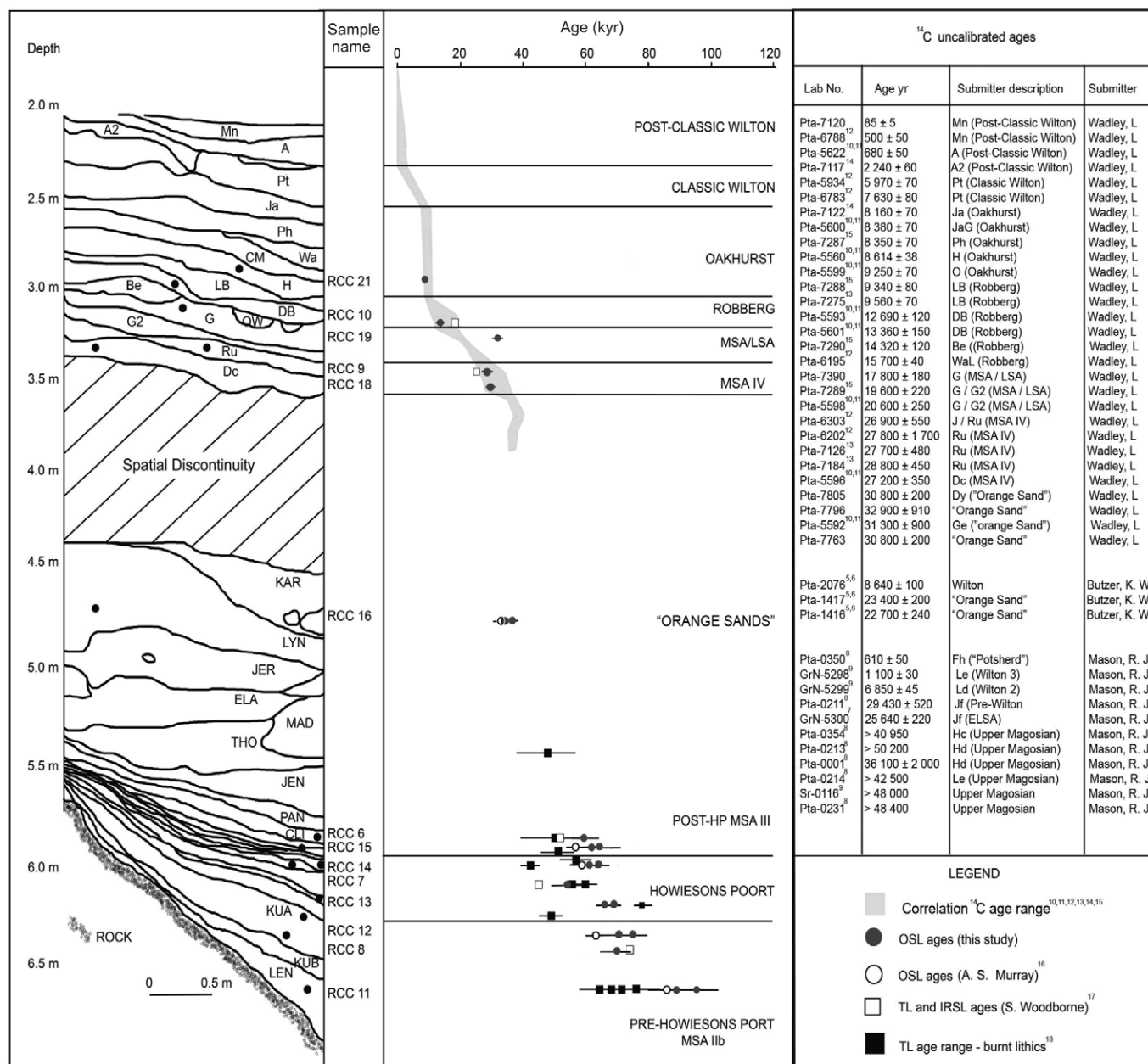


Fig. 1. Sampling strategy and age sequence for Rose Cottage Cave. The LSA stratigraphy is from the Wadley excavation, north section, squares O5 and N5, modified from Clark.¹⁵ The MSA stratigraphy is from the Harper excavation, squares If, Ig and Ih.¹⁶ The LSA chronology was determined on the basis of the ¹⁴C dates, and the MSA chronology was determined using various luminescence techniques.

remove the carbonates and iron, and organics were removed with NaOH. The samples were then dried and bulk sieved into 106–150 μm and 180–212 μm size fractions, depending on their grain size distribution. Magnetic particles were removed using a Franz magnetic separator. A sodium polytungstate solution of specific gravity 2.62 was used for the separation of quartz^{1,20} and feldspars²¹ on the basis of their density. The samples analysed at Risø received no further pre-treatment, whereas those analysed in Pretoria were etched in 40% hydrofluoric acid (HF) to remove any contribution from alpha radiation and any remaining plagioclase feldspars. For each sample the quartz grains were mounted on 24 aluminium disks (aliquots) using silicone oil and the D_e values determined according to the SAR protocol.⁴ Preheats ranged between 160°C and 300°C for 10 s and a cut-heat of 160°C for 0 s was applied. The L_x and T_x OSL signals were stimulated at 125°C for 40 s with blue light-emitting diodes (LEDs) at 90% power. Measurements were carried out on a Risø

automated OSL/TL DA-15 reader. This instrument has both infrared and blue LED stimulation systems and infrared and green laser systems for single-grain measurement. A green long-pass GG-420 filter was installed in front of the blue stimulation diode clusters.²² Both IR and blue diode arrays were equipped with optical feedback systems that stabilized their emission power.²² The ⁹⁰Sr/⁹⁰Y source was calibrated by using gamma-irradiated (5 Gy) calibration quartz (180–212 μm) giving ~10.9 Gy/min. A systematic error for the reader was determined from the error of 10 sequential measurements of an aliquot subjected to a fixed irradiation and measurement protocol. This gave a value of 1.8%.

Assessing the equivalent dose (D_e) determinations
See Appendix 1.

Assessing the dose rate determinations
See Appendix 2.

Table 3. D_e values used in age determination.

Sample name	Sample layer	Archaeological affiliation	D_e values (Gy)*	Age 1 (kyr)*	Age 2 (kyr)*
RCC 21	H	Oakhurst	17.0 ± 1.0		8.6 ± 0.6
RCC 10	DB	Robberg	25.1 ± 2.0	13.6 ± 1.4	13.0 ± 1.2
RCC 19	G	MSA/LSA transition	64.4 ± 1.6	31.7 ± 1.8	
RCC 9	Ru	MSA IV	61.0 ± 2.8	27.6 ± 2.3	
RCC 18	Dc	MSA IV	67.8 ± 2.6		29.8 ± 1.6
RCC 16	LYN	'Sterile sands'	65.0 ± 3.0	34.8 ± 2.2	35.8 ± 2.4
RCC 6	CLI	Post-Howiesons Poort MSA III	102.7 ± 3.1	59.4 ± 4.5	
RCC 15	ANN	Post-Howiesons Poort MSA III	130.0 ± 3.0	61.8 ± 2.8	64.1 ± 2.7
RCC 14	ETH	Howiesons Poort	122.0 ± 3.0	62.5 ± 2.9	64.1 ± 3.0
RCC 7	BER	Howiesons Poort	127.6 ± 3.8	54 ± 4.4	
RCC 13	EMC	Howiesons Poort	133.0 ± 2.0	68.7 ± 2.7	66.9 ± 2.6
RCC 12	KUA	Pre-Howiesons Poort MSA IIb	122.0 ± 4.0	71.4 ± 4.2	74.2 ± 4.2
RCC 8			143.9 ± 5.7	68.6 ± 5.6	
RCC 11	LEN	Pre-Howiesons Poort MSA IIb	158.0 ± 7.0	95.9 ± 6.6	

*The dosimetry is based on U and Th measurements from TSAC (Age 1) and U and Th measurements from the FGS (Age 2). All %K measurements are from XRF analysis.

OSL dates

The OSL results in Tables 3 and 4 and are presented graphically in relation to the stratigraphy in Fig. 1. This includes previous luminescence dates obtained by IRSL, TL^{17,18} and OSL¹⁶ techniques.

Discussion

The younger OSL samples can be compared with the corresponding ¹⁴C dates, but the comparison is not direct. OSL ages are calculated in true calendar years, and the age is reported relative to the calendar date of the analysis. ¹⁴C dates, by contrast, are relative to the year AD 1950, and the age is calculated using the Libby half-life for ¹⁴C, which is known to be in error by approximately 3%.³⁷ This means that '¹⁴C years' are not the same as 'luminescence years'. An additional level of complexity arises from natural fluctuations in the production of ¹⁴C in the atmosphere. Both the secular variation in ¹⁴C and the error resulting from the incorrect half-life used in ¹⁴C dating are accommodated in the 'calibration' of ¹⁴C dates. In this process, the measured ¹⁴C date is compared with ¹⁴C dates from tree rings of known age in order to determine the calendar age of the sample. It became clear recently that differences in carbon cycling in the northern and southern hemispheres gives an approximate 40 year apparent age to the southern hemisphere. This has to be taken into account in the calibration step for ¹⁴C dates because the tree-ring calibration data set derives entirely from the northern hemisphere. It has been shown³⁸ that using a fixed offset between the northern and southern hemispheres is erroneous and calibration of the southern hemisphere is therefore best achieved on dendro-chronologically dated wood. Unfortunately, no such data set exists for the southern hemisphere for the period before 1000 years ago. Furthermore, the calibration record between 26 kyr and 50 kyr ago is constructed from a variety of data sets such as laminated lake sediments, corals and speleothems. There are offsets greater than 2000 years between these data sets.³⁹ The calibration step is nevertheless important and the consistent use of one calibration data set may produce errors in this time range, but the errors will be consistent between different calibrated ¹⁴C dates.

The RCC ¹⁴C dates in this study were calibrated using the southern hemisphere 1998 calibration data set (SH98).⁴⁰ It should be noted that these data are interpolated on relatively few measurements^{41,42} combined with an average 40 year offset from the northern hemisphere 1998 data set (INTCAL 98).⁴³ Where OSL dates were derived using the SAR protocol, the results were compared with the RCC ¹⁴C chronology (Table 5). In order to compare calibrated ¹⁴C dates with OSL dates, it is necessary to

convert them to the same reference. The term 'correlated ¹⁴C age' in this study refers to calibrated ¹⁴C ages expressed in calendar years relative to AD 2005 (the year in which the OSL dates were performed) in order to make a direct comparison with the OSL dates. Figure 2 presents a more detailed comparison between OSL and ¹⁴C and identifies miscorrelations. Because the ¹⁴C calibration can produce asymmetrical error margins, the one-sigma range is presented in Table 5.

Without the benefit of high-resolution gamma spectrometer measurements (HRGS) we use the comparison between ¹⁴C and OSL dates as an indication of the accuracy of the dosimetry. In particular the effect of the disparate XRF and field gamma spectrometer measurements (FGS) for %K were assessed. The XRF-derived results are consistently better correlated with the radio-carbon chronology than the FGS derived measurement (not shown), which suggests that there is a problem with the calibration of the FGS. A further comparison was made between the U and Th dose contribution determined from the FGS and TSAC (see Table 3). This difference was not substantial and the conclusion is that the stripping of the gamma spectra was incorrect for the K channel, and correct for the U and Th channels. Only dates based on the XRF dosimetry were further analysed. Table 3 sum-

Table 4. Ages obtained from previous luminescence studies at RCC.

Sample name	Sample layer	Archaeological affiliation	Luminescence age (kyr)
RCC 10 ¹⁷	DB	Robberg	19.7*
RCC 9 ¹⁷	Ru	MSA IV	20.4*
RCC 16	LYN	'Sterile sands'	33 ± 2
RC 10 ¹⁸	THO	'Sterile sands'	47.1 ± 10.2
RCC 6 ¹⁷	CLI	Post-Howiesons Poort MSA III	48.9*
RC 12 ¹⁸	CLI	Post-Howiesons Poort MSA III	49.4 ± 10.1
RCC 15 ¹⁶	ANN	Post-Howiesons Poort MSA III	57 ± 3
RC 5 ¹⁸	BYR	Post-Howiesons Poort MSA III	50.5 ± 4.6
RC 65 ¹⁸	SUZ	Howiesons Poort	58.6 ± 6.6
RCC 14 ¹⁶	ETH	Howiesons Poort	59 ± 4
RC 36 ¹⁸	ETH	Howiesons Poort	41.7 ± 3.7
RCC 7 ¹⁷	BER	Howiesons Poort	45.4*
RC 41 ¹⁸	BER	Howiesons Poort	56.3 ± 4.5
RC 42 ¹⁸	BER	Howiesons Poort	60.4 ± 4.6
RCC 13 ¹⁶	EMC	Howiesons Poort	66 ± 4
RC 52 ¹⁸	EMD	Pre-Howiesons Poort MSA IIb	48.9 ± 5.3
RCC 8 ¹⁷	KUA	Pre-Howiesons Poort MSA IIb	78.0*
RCC 12 ¹⁶	KUA	Pre-Howiesons Poort MSA IIb	62 ± 4
RCC 11 ¹⁶	LEN	Pre-Howiesons Poort MSA IIb	86 ± 6
RC 54 ¹⁸	LEN	Pre-Howiesons Poort MSA IIb	72.5 ± 6.8
RC 57 ¹⁸	LEN	Pre-Howiesons Poort MSA IIb	76.3 ± 14.8
RC 61 ¹⁸	LEN	Pre-Howiesons Poort MSA IIb	68.4 ± 8.3
RC 62 ¹⁸	LEN	Pre-Howiesons Poort MSA IIb	64.5 ± 6.6

*Represents the consensus age obtained by S. Woodborne.¹⁷

marizes the final D_e values and dose rates that were used to calculate the depositional age of the RCC.

Of the OSL-dated samples that have associated radiocarbon dates, RCC 16, RCC 18 and RCC 9 overlap within the 1-sigma error range, whereas RCC 10 and RCC 21 (using single-grain analysis) overlap at the 2-sigma range. The age of RCC 19 is overestimated by approximately 30% and it is anomalous in the depth/age relationship established from both the radiocarbon and OSL chronologies (see Fig. 1). The result for RCC 19 is particularly unsatisfactory as the OSL analysis for this sample presents perhaps the most convincing case for an acceptable date. The D_e values appear to indicate a single population with minimal scatter around the central value. Such an age discrepancy may result from localized turbation (such as pit digging) that would have elevated older sediments to the surface without necessarily zeroing the OSL signal, or the problem may relate to sampling problems associated with fine stratigraphy (the sampling tube was 30 cm long and 5 cm in diameter), but these seem unlikely. A more likely scenario is that this sample was contaminated with feldspar in the same way that the single-aliquot analysis of RCC 21 was. In the case of RCC 21, the overdispersal of D_e values (15.8%) (discussed in Appendix 1) prompted the single-grain analysis, but because RCC 19 had a low overdispersion value of 7.2%, the possibility of feldspar contamination was not initially considered, and a single-grain analysis was not performed.

The overall correlation between the radiocarbon chronology and the OSL chronology in the upper RCC sequence gives some confidence that the OSL dates from the pre- ^{14}C Middle Stone Age layers are accurate. However, it is noted that RCC 7 yields a date that is younger than those stratified above it (RCC 14, 15 and 6). For this sample either the dose rate is overestimated or the D_e value is underestimated. The SAR protocol that is used to measure the D_e value fails when the OSL/dose-response curve saturates. RCC 7's is the only growth curve in this study that showed evidence of saturation at approximately 150 Gy, so that the D_e value of 127 Gy may be an underestimate. Alternatively, the underestimate of age for RCC 7 may be the result of an overestimation of the dose rate. Previous studies¹³ suggested that RCC has been a chemically dynamic environment. No bone is preserved in these layers and the stratigraphic section shows that the deposit has deformed substantially through profile compaction and leaching. Several age underestimates are noted in other dating studies of the MSA layers using different luminescence techniques and datable materials (Table 4) and it is possible that dosimetry presents a problem. This has not been demonstrated but the result for RCC 7 is rejected as an outlier.

Conclusion

The most probable ages for RCC, presented in Table 6, reflect combined OSL and ^{14}C age ranges that have been calibrated and presented in years before AD 2005. It should be noted that the age

Table 5. ^{14}C /OSL comparison: the correlation age is given as the calibrated 1-sigma ^{14}C age range corrected to years before AD 2005.

Layer	Sample name	Uncalibrated ^{14}C		Correlation age	OSL age
H	RCC 21	8 614 ± 38	(Pta 5560) ^{10,11}	9 582–9 603	8 600 ± 600
DB	RCC 10	12 690 ± 120	(Pta 5593) ^{10,11}	15 023–15 339	13 600 ± 1 400
		13 360 ± 150	(Pta 5601) ^{10,11}	15 869–16 227	13 000 ± 1 200
G	RCC 19	17 800 ± 180	(Pta 7390)	20 953–21 367	31 700 ± 1 800
		19 600 ± 220	(Pta 7289) ¹⁵	22 753–23 126	
		20 600 ± 250	(Pta 5598) ^{10,11}	23 554–23 926	
Ru	RCC 9	26 900 ± 550	(Pta 6303) ¹²	27 832–28 883	27 600 ± 2 300
		27 800 ± 1 700	(Pta 6202) ¹²	27 626–34 515	
		27 700 ± 480	(Pta 7126) ¹³	28 637–29 899	
		28 800 ± 450	(Pta 7184) ¹³	30 243–33 962	
Dc	RCC 18	27 200 ± 350	(Pta 5596) ^{10,11}	28 275–29 001	29 800 ± 1 600
LYN	RCC 16	30 800 ± 200	(Pta 7805)	36 148–36 604	34 800 ± 2 200
		30 800 ± 200	(Pta 7763)	36 148–36 604	35 800 ± 2 400
		31 300 ± 900	(Pta 5592) ^{10,11}	35 905–37 873	
		32 100 ± 910	(Pta 7796)	36 812–38 738	

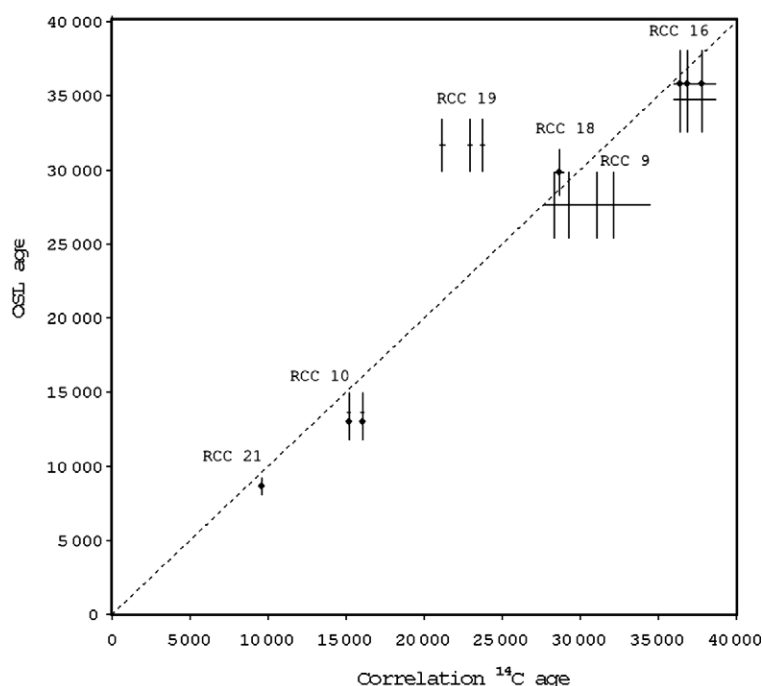


Fig. 2. Comparison between OSL and ^{14}C ages taken from Table 5. Dates are presented in years before AD 2005, and cross lines represent dates derived from Age 1, and dots represent dates from Age 2 (see Table 3).

ranges obtained for RCC are the most probable. To fine-tune these results, further study will need to be conducted focusing on the dosimetry and effect of feldspars. The values in Table 6 are rounded to the nearest 500 years and exclude outliers from both the ^{14}C and OSL chronology. The transition between the Robberg and MSA/LSA transition at RCC is clearly defined at 20 000 years ago by ^{14}C dates. The final MSA at RCC is currently dated to 27 000 years ago by both ^{14}C and luminescence chronologies. The MSA/Early Later Stone Age transition at Border Cave is placed at 41 000 years ago and the final ELSA are at about 30 000 years ago (calibrated relative to AD 2005).⁴⁴ The corresponding period at RCC is represented by the top of the 'almost sterile' orange sand through to the layers classified as MSA IV by Wadley.¹⁰ This focuses attention on the RCC 19 OSL date of 31.7 kyr, which is rejected on the basis of the other OSL dates stratified above and below it as well as the ^{14}C dates. A literal acceptance of this date would shift the MSA/LSA transition at RCC closer to the age range defined at Border Cave. If it is shown

Table 6. Most probable age ranges for the Rose Cottage Cave sequence. The ages exclude outliers from both the OSL and radiocarbon chronologies.

Archaeological affiliation	Probable age range (calendar years ago relative to AD 2005)
Post-Classic Wilton	<3 000
Classic Wilton	3 000–8 500
Oakhurst	8 600–10 500
Robberg	10 500–20 000
MSA/LSA transition	20 000–27 000
MSA IV	>27 000–35 000
'Orange sand'	~35 000
Post-Howiesons Poort MSA III	>35 000– <60 000
Howiesons Poort	60 000–70 000
Pre-Howiesons Poort MSA IIb	70 000–96 000

that RCC 19 is contaminated with feldspar as has been suggested here, then the date is an overestimation of the MSA/LSA, and the ^{14}C chronology will stand. The latter interpretation is the simplest explanation of the data, and is supported by the similarity in stone tool assemblages from the MSA IV stone tool assemblage dated to between approximately 38 000 years ago and 27 000 years ago (layers LYN to Ru) with those defined as ELSA at Border Cave.^{44,45}

Published dates for Howiesons Poort assemblages in South Africa range between approximately 80 000 and 50 000 years ago.^{16,18,46–50} As the dating techniques improve, this range is likely to narrow. Unfortunately, a largely random scatter in the previous Howiesons Poort dates from RCC undermines their credibility, and it is likely that problems of feldspar contamination are the underlying cause. With the improvement in the SAR OSL dating technique, the results are significantly improved, and this study yields a coherent set of OSL dates that place the Howiesons Poort between 70 000 and 60 000 years ago.

Received 11 August 2006. Accepted 17 November 2007.

- Huntley D.J., Hutton J.T. and Prescott J.R. (1993). The stranded beach-dune sequence of south-east South Australia: a test of thermoluminescence dating, 0–800 ka. *Quat. Sci. Rev.* **12**, 1–20.
- Singarayer J.S., Bailey R.M., Ward S. and Stokes S. (2001). Assessing the completeness of quartz OSL in the natural environment. *Radiation Measurements* **40**, 13–25.
- Bailey R.M. (2003). The use of measurement-time dependent single-aliquot equivalent-dose estimates from quartz in the identification of incomplete signal resetting. *Radiation Measurements* **37**, 673–683.
- Murray A.S. and Wintle A.G. (2000). Luminescence dating of quartz using an improved single-aliquot regenerative-dose protocol. *Radiation Measurements* **32**, 57–73.
- Butzer K.W. (1984). In *Late Cainozoic Palaeoclimates of the Southern Hemisphere*, ed. J.C. Vogel, pp. 235–264. Balkema, Rotterdam.
- Butzer K.W. (1984). In *Southern African Prehistory and Palaeoenvironments*, ed. R.G. Klein, pp. 1–64. Balkema, Rotterdam.
- Vogel J.C. (1970). Groningen radiocarbon dates. IX. *Radiocarbon* **12**, 444–471.
- Vogel J.C. and Marais M. (1971). Pretoria radiocarbon dates. *Radiocarbon* **1**, 387–394.
- Beaumont P.B. and Vogel J.C. (1972). On a new radiocarbon chronology for Africa south of the Equator, Part 1. *Afr. Stud.* **31**, 65–89.
- Wadley L. (1991). Rose Cottage Cave: background and a preliminary report on the recent excavations. *S. Afr. Archaeol. Bull.* **46**, 125–130.
- Wadley L. and Vogel J.C. (1991). New dates from Rose Cottage Cave, Ladybrand, eastern Orange Free State. *S. Afr. J. Sci.* **87**, 605–608.
- Wadley L. (2005). Review of dated Stone Age sites recently excavated in the eastern Free State, South Africa. *S. Afr. J. Sci.* **91**, 574–579.
- Woodborne S. and Vogel J.C. (1997). Luminescence dating at Rose Cottage Cave: a progress report. *S. Afr. J. Sci.* **93**, 467–470.
- Wadley L. (1997). Rose Cottage Cave: archaeological work 1987 to 1997. *S. Afr. J. Sci.* **93**, 439–447.
- Clark A.M.B. (1999). Late Pleistocene technology at Rose Cottage Cave: a search for modern behaviour in an MSA context. *Afr. Archaeol. Rev.* **16**, 93–119.
- Cochrane G.W. (2004). *The role of diversity in the evolution of symbolic behaviour: insights from South African lithic assemblages*. Ph.D thesis, University of the Witwatersrand, Johannesburg.
- Woodborne S. (1999). *Dating the Middle Stone Age in South Africa*. National Research Foundation Final Report: 15/1/3/2/00231. Pretoria.
- Valladas H., Wadley L., Mercier N., Froget L., Tribolito C., Reyss J.L. and Joron J.L. (2005). Thermoluminescence dating on burnt lithics on Middle Stone Age layers at Rose Cottage Cave. *S. Afr. J. Sci.* **101**, 169–174.
- Wintle A.G. and Murray A.S. (2006). A review of quartz optically stimulated luminescence characteristics and their relevance in single-aliquot regeneration dating protocols. *Radiation Measurements* **41**, 369–391.
- Stokes S. (1992). Optical dating of young (modern) sediments using quartz: results from a selection of depositional environments. *Quat. Sci. Rev.* **11**, 153–159.
- Mejdahl V. (1985). Thermoluminescence dating of partially bleached sediments. *Nuclear Tracks and Radiation Measurements* **10**, 711–715.
- Bøtter-Jensen L., Andersen C.E., Duller G.A.T. and Murray A.S. (2003). Developments in radiation, stimulation and observation facilities in luminescence measurements. *Radiation Measurements* **37**, 535–541.
- Wallinga J., Murray A.S., Duller G.A.T. and Törnqvist T.E. (2001). Testing optically stimulated luminescence dating of sand-sized quartz and feldspar from fluvial deposits. *Earth Planet. Sci. Lett.* **193**, 617–630.
- Murray A.S. and Roberts R.G. (1998). Measurement of the equivalent dose in quartz using a regenerative-dose single-aliquot protocol. *Radiation Measurements* **29**, 503–515.
- Roberts R.G., Galbraith R.F., Olley J.M., Yoshida H. and Laslett G. (1999). Optical dating of single and multiple grains of quartz from Jinmium rock shelter, northern Australia: Part II, Results and implications. *Archaeometry* **41**, 365–395.
- Aitken M.J. and Smith B.W. (1988). Optical dating: recuperation after bleaching. *Quat. Sci. Rev.* **7**, 387–393.
- Murray A.S. and Olley J.M. (2002). Precision and accuracy in the optically stimulated luminescence dating of sedimentary quartz: a status review. *Geochronometria* **21**, 1–16.
- Aitken M.J. (1998). *An Introduction to Optical Dating*. Oxford University Press, Oxford.
- Duller G.A.T. (2003). Distinguishing quartz and feldspar in single grain luminescence measurements. *Radiation Measurements* **37**, 161–165.
- Jacobs Z., Wintle A.G. and Duller G.A.T. (2003). Optical dating of dune sand from Blombos Cave, South Africa: I – multiple grain data. *J. Hum. Evol.* **44**, 599–612.
- Jacobs Z., Wintle A.G. and Duller G.A.T. (2006). Evaluation of SAR procedures for D_e determination using single aliquots of quartz from two archaeological sites in South Africa. *Radiation Measurements* **41**, 520–533.
- Wintle A.G. and Murray A.S. (1998). Towards the development of a preheat procedure for OSL dating of quartz. *Radiation Measurements* **29**, 81–94.
- Galbraith R.F., Roberts R.G., Laslett G.M., Yoshida H. and Olley J.M. (1999). Optical dating of single and multiple grains of quartz from Jinmium rock shelter, northern Australia: Part I, Experimental design and statistical models. *Archaeometry* **41**, 339–364.
- Adamiec G. and Aitken M.J. (1998). Dose-rate conversion factors: update. *Ancient TL* **16**, 37–49.
- Rees-Jones J. (1995). Optical dating of young sediments using fine-grain quartz. *Ancient TL* **13**, 9–14.
- Wadley L. (1996). The Robberg industry of Rose Cottage Cave, Eastern Free State: the technology, spatial patterns and environment. *S. Afr. Archaeol. Bull.* **51**, 64–74.
- Stuiver M. and Polach H.A. (1977). Discussion: Reporting of ^{14}C data. *Radiocarbon* **19**, 355–363.
- McCormac F.G., Hogg A.G., Blackwell P.G., Buck C.E., Higham T.F.G. and Reimer P.J. (2004). SHCAL04 Southern Hemisphere Calibration, 0–11.0 cal kyr BP. *Radiocarbon* **46**, 1087–1092.
- Van der Plicht J., Beck J.W., Bard E., Baillie M.G.L., Blackwell P.G., Buck C.E., Friedrich M., Guilderson T.P., Hughen K.A., Kromer B., McCormac F.G., Bronk Ramsey C., Reimer P.J., Reimer R.W., Remmele S., Richards D.A., Southon J.R., Stuiver M. and Weyhenmeyer C.E. (2004). NOTCAL04 – Comparison/Calibration ^{14}C records 26–50 cal kyr BP. *Radiocarbon* **46**, 1225–1238.
- Stuiver M., Reimer P.J. and Braziunas T.E. (1998). High-precision radiocarbon age calibration for terrestrial and marine samples. *Radiocarbon* **40**, 1127–1151.
- Talma A.S. and Vogel J.C. (1992). Late Quaternary palaeotemperatures derived from a speleothem from Congo Cave, Cape Province, South Africa. *Quat. Res.* **37**, 203–213.
- Talma A.S. and Vogel J.C. (1993). A simplified approach to calibrating ^{14}C dates. *Radiocarbon* **35**, 317–322.
- Stuiver M., Reimer P.J., Bard E., Beck J.W., Burr G.S., Hughen K.A., Kromer B., McCormac F.G., Van der Plicht J. and Spurk M. (1998). IntCal98 radiocarbon age calibration, 24 000–0 cal BP. *Radiocarbon* **40**, 1041–1083.
- Grün R. and Beaumont P. (2001). Border Cave revisited: a revised ESR chronology. *J. Hum. Evol.* **40**, 467–482.
- Bird M.L., Fifield L.K., Santos G.M., Beaumont P.B., Zhou Y., Di Tada M.L. and Hausladen P.A. (2003). Radiocarbon dating from 40 to 60 ka BP at Border Cave, South Africa. *Quat. Sci. Rev. (Quat. Geochronol.)* **22**, 943–947.
- Feathers J. K. (2002). Luminescence dating in less than ideal conditions: case studies from Klasies River Mouth and Duinefontein, South Africa. *J. Archaeol. Sci.* **29**, 177–194.
- Grün R. and Beaumont P. B. (2001). Border Cave revisited: a revised ESR chronology. *J. Hum. Evol.* **40**, 467–482.
- Grün R., Shackleton N. J. and Deacon H. J. (1990). Electron-spin resonance dating from Klasies River Mouth Cave. *Curr. Anthropol.* **32**, 427–432.
- Miller G. H., Beaumont P. B., Deacon H. J., Brooks A. S., Hare P. E. and Jull A. J. T. (1999). Earliest modern humans in South Africa dated by isoleucine epimerization in ostrich eggshell. *Quat. Sci. Rev.* **18**, 1537–1548.
- Tribolo C. (2003). *Apport des méthodes de la luminescence à la chronologie des techno-facies du Middle Stone Age associés aux premiers hommes modernes du Sud de l'Afrique*. D.Phil. thesis, University of Bordeaux I.

51. Vogel J. C. (2000). Radiometric dates for the Middle Stone Age in South Africa. In *Humanity from African Naissance to Coming Millennia*, eds P.V. Tobias, M.A. Raath, J. Moggi-Cecchi and G.A. Doyle, pp. 261–268. University of Florence Press, Florence.

This article is accompanied by supplementary tables and figures online at www.sajs.co.za

Appendix 1

Assessing the equivalent dose (D_e) determinations

Aliquots from samples RCC 6–10, 18, 19 and 21 were assessed against OSL rejection criteria that were assumed to eliminate most errors derived from the OSL behaviour and sedimentary history of the grains (see Table 1 in supplementary material online). The first and probably the most important test is termed the *dose recovery test*.²³ If the SAR protocol is applied to grains that are artificially irradiated with a known dose and it does not yield that dose (a laboratory dose is not recovered), there is a high probability that the equivalent dose (D_e) will be inaccurate. Dose recovery experiments^{24,25} were performed on six aliquots per sample. The aliquots were optically bleached using blue LEDs for 40 s at 125°C. After zeroing, a known laboratory dose assumed to be representative of the equivalent dose was administered and a conventional SAR protocol was performed using a preheat of 240°C and a cut heat of 160°C to see if the dose could be recovered. The recovery ratios were above 0.98 with the exception of sample RCC 8, which gave a 0.92 ± 0.01 recovery ratio.

Recuperation, or ‘charge transfer’, is the trapping of electrons in the OSL-related traps when they are ejected from non-OSL traps during heat treatment (preheating). This phenomenon can result in unacceptable variability in D_e values.²⁶ Recuperation was tested by expressing the ratio between an additional zero dose OSL signal and the natural OSL signal as a percentage of the natural $[(L_g/T_5)/(L_1/T_1)]$. All values greater than 5% were rejected.²⁷ No samples from RCC had recuperation values greater than 1.5%.

Scatter in the equivalent dose measurements can result from feldspar grains that have not been eradicated during pre-treatment. Feldspar contamination in quartz aliquots can result in overestimated D_e values because of the potassium contribution to the internal dose, or it can result in an underestimation of D_e if anomalous fading has taken place.²⁸ The OSL IR depletion ratio test²⁹ relies on the depletion of the OSL signal in feldspars under room temperature IR stimulation, whereas quartz is unaffected. Two successive OSL measurements were made with the same applied dose, but with an IR bleaching step (IR diodes set to 90% power for 100 s) before the second OSL measurement. Any depletion of the signal measured would be the result of feldspar contamination. A reduction criterion of more than two standard deviations from unity was used to determine an acceptable ratio of $[(L_1/T_1)/(L_2/T_2)]$.³⁰ Aliquots with an OSL IR depletion ratio below this rejection criterion were assumed to contain feldspar and were omitted from further analysis. Figure A (see supplementary material online) shows the OSL IR depletion ratio test for un-etched aliquots of RCC 6 using a large (5 mm) mask; a 2-mm mask and the results of aliquots of the same sample that was etched in HF acid. Of 408 aliquots in the entire study, 106 (~26%) were rejected due to feldspar contamination. The following analysis is restricted to only the 74% of aliquots that passed the OSL IR depletion ratio test.

The recycling ratio (R-ratio) test was used to check reproducibility within the SAR measurement cycle.⁴ In this study, two regenerative doses were repeated: one with a low dose to mimic the first regenerative point in which most sensitivity changes took place, and a second point with a high dose.³¹ The two recycling ratios $[(L_{x1}/T_{x1})/(L_{x2}/T_{x2})]$ should be very close to unity if appropriate sensitivity corrections during a SAR measurement cycle are applied. In practice, less than two standard deviations from unity is acceptable.³ Most of the aliquots from RCC pass this test, indicating good recycling behaviour.

The test used to establish adequate bleaching is the $D_e(t)$ method.³ This relies on the fact that the OSL signal comprises a thermally stable fast bleaching component and slow bleaching components that can be resolved. If the sample is partially bleached, then the slower bleaching components yield a greater residual signal. This test calculates D_e as a function of stimulation time (using approximately 0.5-second integration channels), and it was performed on samples RCC 6–10, 18, 19 and 21. Ten random aliquots representative of a preheat range between 160°C and 300°C were used for each sample. The results indicated that no partial bleaching had occurred. Partial bleaching would be anticipated with fluvial deposition or weathered spall contamination, and the results seem to indicate a predominantly aeolian mode of deposition (see Fig. B online).

After all rejection criteria⁴ have been met, the remaining aliquots were subject to a preheat plateau test. For each aliquot the D_e value was plotted against preheat temperature to establish if the thermal treatment was too passive and did not adequately remove the unstable signal compo-

nents. This was a test of the appropriateness of the preheat protocol; where a plateau was not established in a given preheat temperature range, all aliquots preheated in that range were rejected.³²

The final assessment was of the distribution of D_e values in the form of over-dispersion values³¹ (see Table 1 online) and a visual assessment in radial and probability density plots. With the exception of RCC 21 (see Fig. C online), all the samples were scattered evenly around a central mean so the central age model was used³³ to determine the D_e values. Because of its asymmetric D_e distribution, RCC 21 was selected for single-grain analysis (see Fig. D online). This method used the same protocol as the multi-grain aliquots except that a laser was used to stimulate individual grains. The logic behind the single-grain analysis is to separate different populations of grains from a sample of mixed age and in this way explain the observed over-dispersion. A total of 1000 grains were analysed, but in the case of RCC 21 the analysis did not show a mixed population. Instead, over 50% of grains were rejected due to feldspar contamination when using the OSL IR depletion ratio test.²⁹ This is surprising as the same fraction of pre-treated grains was used to make the single-aliquot and the single-grain analyses, and only one of the 24 single aliquots was rejected on this criterion. The HF etch appeared not to have removed all feldspars, but the IR-depletion test on the aliquots did not identify the problem with any accuracy. The result of the single-grain analysis indicated that the high D_e values in the single-aliquot analysis were the result of feldspar contamination. It is not clear why the feldspar test was more effective using laser stimulation on individual grains than using diode stimulation on aliquots. Because the single aliquots for RCC 21 must also have contained feldspar, and the feldspars led to D_e overestimations, it was more appropriate to apply a minimum age model.³³ This yielded a D_e value of 16.3 Gy, which corresponds well with the single-grain value of 17.0 ± 1.0 Gy.

Appendix 2

Assessing the dose rate determinations

The dose rate was measured using a variety of methods. Thick source alpha counting (TSAC) analyses were done in the Pretoria laboratory, field gamma spectrometer measurements (FGS) were conducted for some of the samples with an Aptec system at the time of sampling, and high-resolution gamma spectrometer measurements (HRGS) were performed on a set of samples sent to Denmark for analysis by A.S. Murray.¹⁴ Bulk potassium was measured by X-ray fluorescence (XRF) analysis by a commercial subcontracted laboratory (Setpoint). The element concentrations of uranium, thorium and potassium were converted into dose rates using the method outlined by Adamiec and Aitken³⁴ using an assumed average water content of $5 \pm 5\%$ and an alpha efficiency (where appropriate) of 0.04 ± 0.02 .³⁵ The moisture content for RCC was measured between 1% and 3%, but it is assumed that this was not the average value over the depositional history of the site. The large error in the water content estimation is assumed to cover the range of variability that might have occurred had the site been substantially wetter than the present from time to time.

The %K values obtained by FGS and XRF analysis did not always produce the same results (see Table 2 online). Potassium feldspar was found in relatively high concentrations throughout the site and the average contribution of ⁴⁰K to the total dose rate for all samples was 65%. The large contribution from ⁴⁰K to the dose rate limits the effects of the Th and U measurement error in the total environmental dose rate, but it amplified the discrepancy between %K values determined by different techniques. Where there were both XRF and FGS measurements for samples, the FGS/XRF ratio was calculated (Table 2). The ratios averaged at $0.86 \pm 0.13\%$. The XRF technique measured the average K concentration of the bulk sample taken back to the laboratory, whereas FGS integrated the gamma spectrum from a sphere of approximately 30 cm radius *in situ* in the locale from which the sample was removed. A possible cause might be the inhomogeneous distribution of K due to the large numbers of hearths present in the archaeological record.^{10,36} The two approaches may have measured different things, but if this was the cause of the discrepancy then a random distribution of FGS/XRF ratios might be anticipated. Alternatively, a consistently biased error may have arisen from systematic errors in either the FGS or XRF.

The contribution of alpha radiation is assumed to be negligible on samples that were subject to HF etching. The result from single-grain analysis of RCC 21 illustrates that feldspars were not entirely removed by the HF treatment and the possibility that the outer surface of quartz grains was not completely etched must be considered. Where both etched and un-etched material was analysed, the latter was preferred on the basis of the better dosimetry. Only sample RCC 8 produced a statistically distinct date using the etched and un-etched material, and the latter was more closely aligned with RCC 12 date from the same layer.

Supplementary material to:

Pienaar M., Woodborne S. and Wadley L. (2008). Optically stimulated luminescence dating at Rose Cottage Cave *S. Afr. J. Sci.* **104**, 65–69.

Table 1. D_e rejection criteria for RCC samples. The samples are listed in order of depth; samples RCC 6–10 include tests performed on 2-mm and 5-mm mask sizes. The numbers below the IR-OSL and R-ratio columns represent the number of aliquots that were sequentially rejected (left to right) from the initial 24 aliquots. When the number of rejected aliquots was too large no further analysis was carried out. Presented under the preheat plateau column is the number of rejected aliquots range followed by the temperature range that was rejected. Samples RCC 11–16 were analysed in Risø, Denmark, by A.S. Murray¹⁶ and only the D_e estimates are available.

Sample name	Layer name	Mask size (mm)	HF etch	Dose recovery ratio	IR-OSL	R-ratio 1	R-ratio 2	Preheat plateau	D_e (Gy)	Overdispersion (%)
RCC 21	H	2	Y		1	2	1	2, 300°	20.2 ± 0.8	15.8
		Single grain	Y		500	240	NA	NA	17.0 ± 1.0	20.4
RCC 10	DB	5	N		24					
		2	N		4	2	0	8, 260°–300°	25.1 ± 2.0	25.2
			Y	0.98 ± 0.01	0	4	1	10, 160°–220°	27.5 ± 1.1	13.8
RCC 19	G	2	Y		0	0	0	11, 160°–220°	64.4 ± 1.6	7.2
RCC 9	Ru	5	N		0	0	0	0	61.9 ± 1.4	9.8
		2	N		3	4	0	4, 160°, 300°	61.0 ± 2.8	15.6
			Y	98.7 ± 0.03	3	5	0	6, 160°, 180°	59.7 ± 2.0	9.4
RCC 18	Dc	2	Y	100 ± 0.01	0	1	0	2, 300°	67.8 ± 2.6	15.3
RCC 16	Lyn	>5	N						65.0 ± 3.0	
RCC 6	CLY	5	N		24					
		2	N		5	0	0	0	102.7 ± 3.1	12.7
			Y	0.99 ± 0.04	4	1	0	5, 160°, 180°	97.5 ± 4.0	9.1
RCC 15	ANN	>5	N					130.0 ± 3.0		
RCC 14	ETH	>5	N					122.0 ± 3.0		
RCC 7	BER	5	N		22					
		2	N	99.9 ± 0.01	4	2	0	6, 160°, 180°	127.6 ± 3.8	9.1
RCC 13	EMC	>5	N					133.0 ± 2.0		
RCC 12	KUA	>5	N					122.0 ± 4.0		
RCC 8	KUA	5	N		4	0	0	0	139.3 ± 3.7	9.8
		2	N		7	0	0	6, 160°, 280°, 300°	143.9 ± 5.7	13.4
			Y	0.92 ± 0.01	1	2	0	3, 160°	129.2 ± 6.7	20.7
RCC 11	LEN	>5	N					158.0 ± 7.0		

Table 2. Dosimetry for RCC samples. Samples are listed in sequence according to depth.

Sample name	Th (ppm)	U (ppm)	Th/U ratio	Technique*	%K XRF	%K FGS	K ratio (FGS/XRF)	Th + U dose rate (Gy/kyr)	Dose rate 1 (Gy/kyr)	Dose rate 2 (Gy/kyr)
RCC 21	3.33 ± 0.12	0.85 ± 0.04	3.92	FGS	1.55	1.17	0.75	0.459 ± 0.023	1.970 ± 0.033	1.598 ± 0.033
RCC 10	3.43 ± 0.39	1.26 ± 0.04	2.73	TSAC	1.45	1.20	0.83	0.529 ± 0.044	1.847 ± 0.054	1.618 ± 0.054
	3.71 ± 0.12	1.01 ± 0.04	3.68	FGS	1.45	1.20	0.83	0.526 ± 0.024	1.936 ± 0.034	1.691 ± 0.034
	3.09 ± 0.08	1.32 ± 0.04	2.34	TSAC 2	1.45	1.20	0.83	0.520 ± 0.021	1.838 ± 0.030	1.609 ± 0.030
RCC 19	4.22 ± 0.57	1.45 ± 0.06	2.91	TSAC	1.55			0.628 ± 0.062	2.033 ± 0.072	
RCC 9	4.09 ± 0.74	1.40 ± 0.08	2.92	TSAC	1.76			0.608 ± 0.078	2.208 ± 0.088	
	4.10 ± 0.09	1.50 ± 0.03	2.73	TSAC 2	1.76			0.632 ± 0.019	2.232 ± 0.029	
RCC 18	4.29 ± 0.13	1.13 ± 0.05	3.79	FGS	1.72	1.26	0.73	0.600 ± 0.026	2.272 ± 0.036	1.821 ± 0.036
RCC 16	5.05 ± 0.15	1.30 ± 0.04	3.87	TSAC	1.34	1.22	0.91	0.653 ± 0.026	1.870 ± 0.036	1.761 ± 0.036
	3.26 ± 0.14	1.10 ± 0.05	2.97	FGS	1.34	1.22	0.91	0.515 ± 0.028	1.816 ± 0.038	1.700 ± 0.038
RCC 6	3.34 ± 0.68	1.33 ± 0.07	2.51	TSAC	1.26			0.564 ± 0.076	1.730 ± 0.086	
	3.36 ± 0.08	1.39 ± 0.03	2.42	TSAC 2	1.26			0.580 ± 0.019	1.746 ± 0.029	
RCC 15	5.80 ± 0.25	1.53 ± 0.07	3.78	TSAC	1.48	1.14	0.77	0.758 ± 0.041	2.102 ± 0.050	1.845 ± 0.052
	3.64 ± 0.14	1.29 ± 0.06	2.82	FGS	1.48	1.14	0.77	0.590 ± 0.029	2.028 ± 0.039	1.698 ± 0.039
RCC 14	5.55 ± 0.21	1.61 ± 0.06	3.45	TSAC	1.31	1.18	0.89	0.757 ± 0.035	1.952 ± 0.045	1.826 ± 0.045
	3.63 ± 0.17	1.44 ± 0.07	2.52	FGS	1.31	1.18	0.89	0.625 ± 0.035	1.903 ± 0.044	1.769 ± 0.044
RCC 7	7.44 ± 1.19	1.46 ± 0.11	5.11	TSAC	1.66			0.856 ± 0.122	2.365 ± 0.131	
	7.47 ± 0.18	1.41 ± 0.03	5.30	TSAC 2	1.66			0.848 ± 0.026	2.357 ± 0.035	
RCC 13	7.15 ± 0.24	1.27 ± 0.07	5.61	TSAC	1.26	1.02	0.81	0.795 ± 0.040	1.937 ± 0.050	1.723 ± 0.050
	3.63 ± 0.18	2.03 ± 0.08	1.79	FGS	1.26	1.02	0.81	0.767 ± 0.038	1.989 ± 0.048	1.761 ± 0.048
RCC 12	4.27 ± 0.21	1.59 ± 0.06	2.69	TSAC	1.15	1.33	1.15	0.664 ± 0.036	1.708 ± 0.046	1.868 ± 0.046
	3.91 ± 0.18	0.95 ± 0.06	4.11	FGS	1.15	1.33	1.15	0.528 ± 0.032	1.645 ± 0.042	1.817 ± 0.042
RCC 8	7.24 ± 0.78	1.80 ± 0.08	4.01	TSAC	1.23			0.961 ± 0.085	2.099 ± 0.095	
	4.91 ± 0.12	0.65 ± 0.02	6.55	TSAC 2	1.23			0.517 ± 0.019	1.655 ± 0.029	
RCC 11	4.09 ± 0.20	1.08 ± 0.06	3.78	TSAC	1.22	1.17	0.95	0.536 ± 0.034	1.648 ± 0.044	1.596 ± 0.044
	3.85 ± 0.15	1.19 ± 0.05	3.22	FGS	1.22	1.17	0.95	0.582 ± 0.030	1.771 ± 0.039	1.716 ± 0.039

*Thick source alpha counting (TSAC) measurements were performed by M. Pienaar (TSAC) and S. Woodborne (TSAC 2). Other measurement procedures include field gamma spectrometry (FGS) and X-ray fluorescence (XRF). Dose rate 1 was calculated from the %K values measured with the XRF, and dose rate 2 was calculated from %K values measured with the FGS. Dose rates presented in bold were used to determine the date range in Table 5.

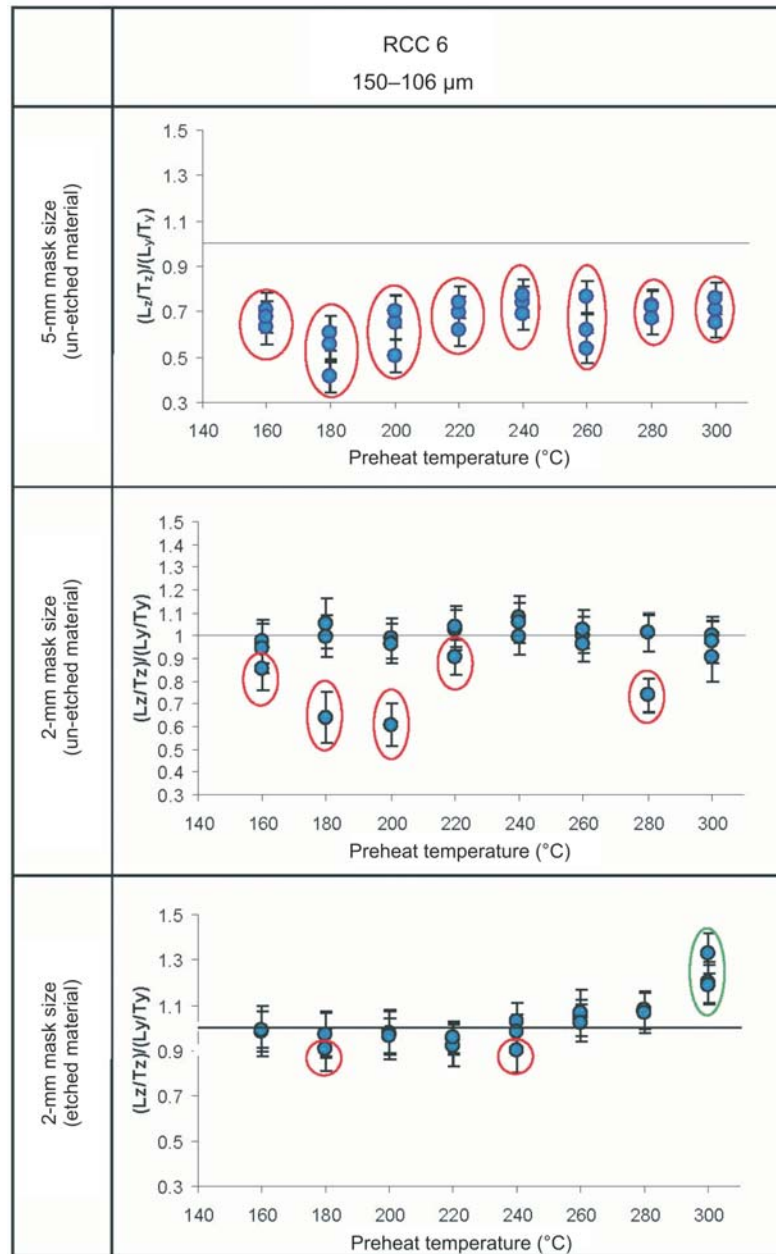


Fig. A. OSL IR depletion ratio tests performed on aliquots using 5-mm and 2-mm mask sizes at different preheat temperatures. The OSL IR depletion ratio²⁹ is given as $[(L_z/T_z)/(L_y/T_y)]$, where L and T are the regenerated OSL intensity of the given dose and the test dose, respectively. Note that two aliquots in the 2-mm mask size (etched material) were rejected due to recycling behaviour rather than feldspar contamination.

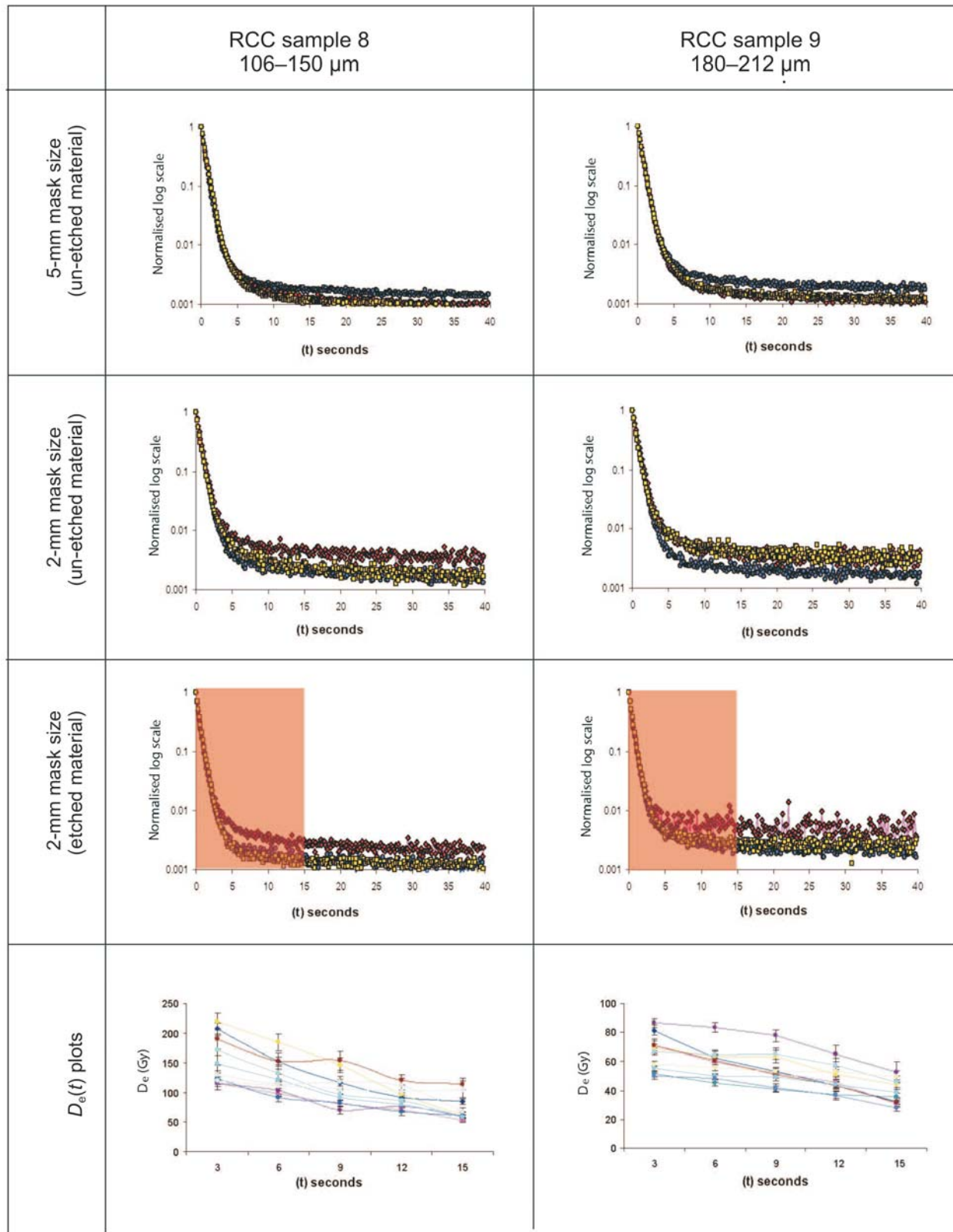


Fig. B. Plots showing the first 40 seconds of OSL decay for aliquots that were accepted for HF etched samples of RCC 8 (MSA) and RCC 9 (LSA). The $D_e(t)$ plots are constructed from the first 15 seconds (shaded areas) of stimulation. The signal used for dating was the integral of the first three seconds. Ten aliquots were used to construct the $D_e(t)$ plots. The downward trend in these plots, as was the case for all other aliquots that were analysed, indicates that the samples were not inadequately bleached.

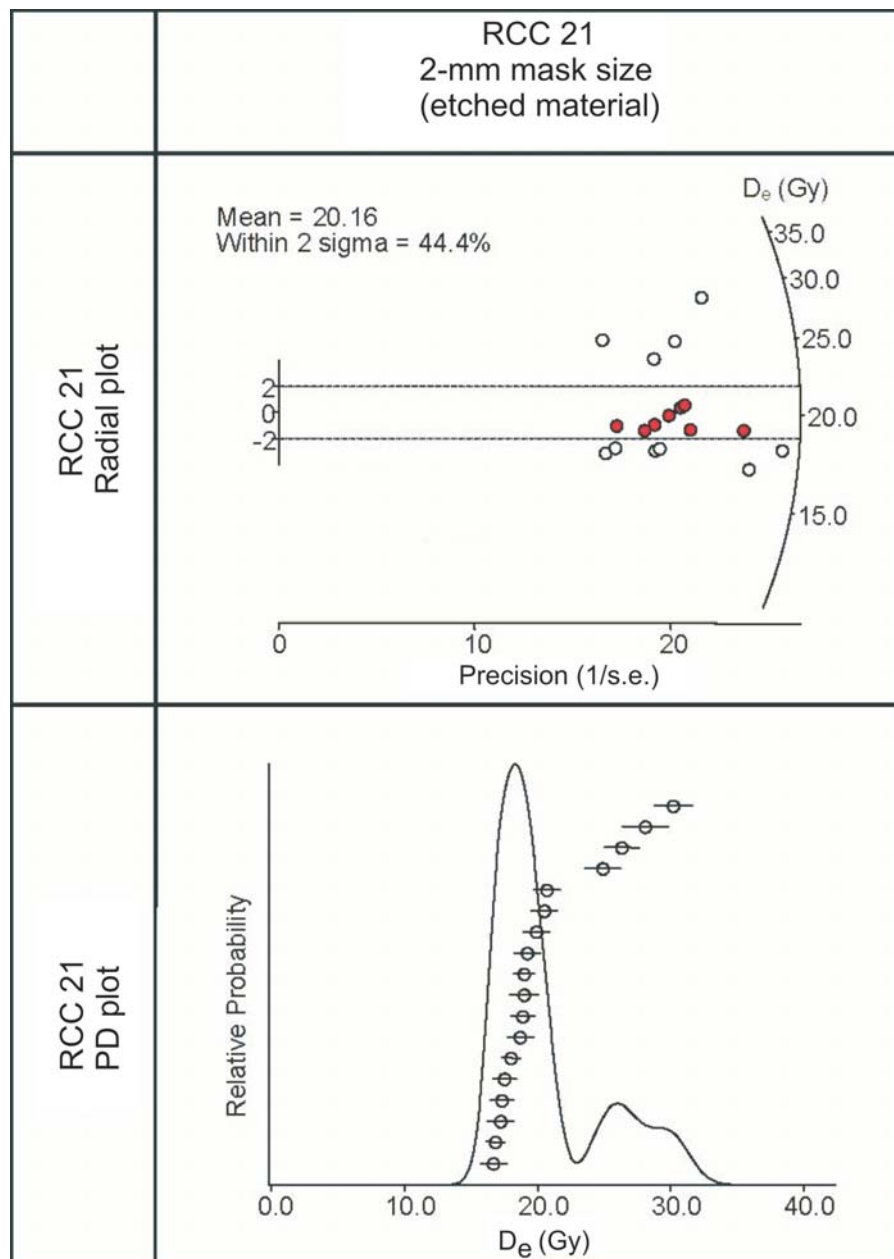


Fig. C. Radial plot and probability density (PD) plot showing the D_e distributions for sample RCC 21 using the SAR approach. A central age model³³ yields a D_e value of 20.2 Gy, but the bimodal distribution suggests at least two populations. Insight from the single-grain analysis of this sample suggests that this is the result of some feldspar contamination, and so a minimum age model³³ was also applied. This yielded a D_e value of 16.3 Gy.

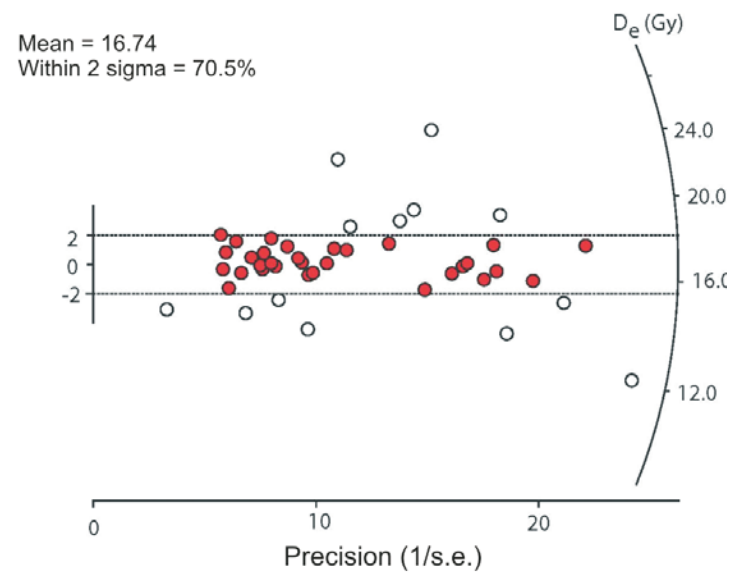
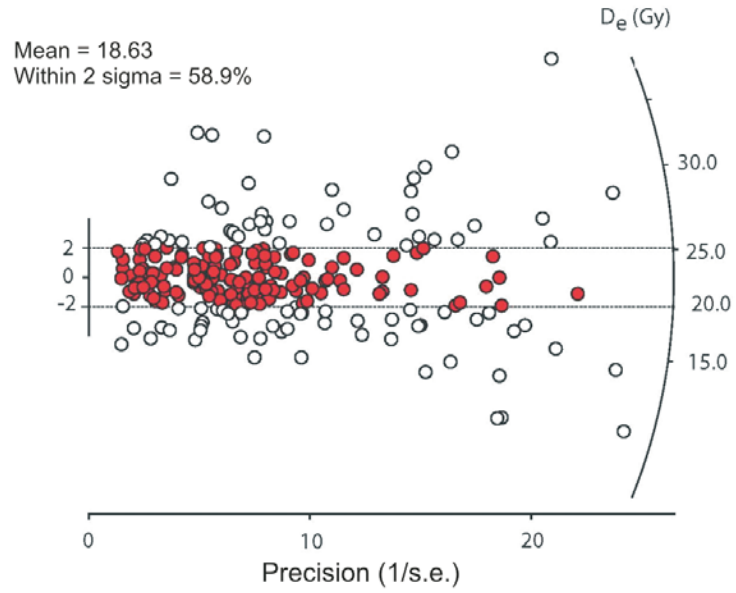


Fig. D. Radial plots showing all the grains (left) and the accepted grains (right) from the single-grain analysis of sample RCC 21. The grains were almost entirely rejected on the basis of feldspar contamination.